INTERNATIONAL JOURNAL OF CLIMATOLOGY
Int. J. Climatol. **32**: 2073–2080 (2012)
Published online 17 June 2011 in Wiley Online Library
(wileyonlinelibrary.com) DOI: 10.1002/joc.2378

RMetS
Royal Meteorological Society

Short Communication

Impacts of tropical Indian Ocean SST on the meridional displacement of East Asian jet in boreal summer

Xia Qu[a,b,c] and Gang Huang[d]*

[a] *Center for Monsoon System Research, Institute of Atmospheric Physics, Chinese Academy of Sciences, Beijing 100029, China*
[b] *Graduate University of Chinese Academy of Sciences, Beijing 100049, China*
[c] *Key Laboratory of Global Change and Marine-Atmospheric Chemistry, the Third Institute of Oceanography State Oceanic Administration, Xiamen 361005, China*
[d] *Key Laboratory of Regional Climate-Environment Research for Temperate East Asia, Institute of Atmospheric Physics, Chinese Academy of Sciences, Beijing 100029, China*

ABSTRACT: The meridional displacement of East Asia jet (EAJ) is characterized by the leading mode of upper tropospheric zonal wind variability over East Asia in boreal summer, and is closely related to the East Asia summer monsoon and downstream climate. Present study reveals that the meridional displacement of EAJ is associated with tropical Indian Ocean (TIO) SST anomalies. When the TIO SST is higher than normal, the overlying tropospheric air warms up through the modulation of the TIO SST on tropical convection. The anomalous convection forces a Kelvin wave wedge penetrating into the equatorial western Pacific, leading to a decrease in precipitation near the Philippines. Combined with the climatological easterly shear over the subtropical western North Pacific, the Pacific-Japan/East Asia-Pacific (PJ/EAP) teleconnection is induced along the East Asia coast. The PJ/EAP-related upper-level anomalous cyclone accelerates westerly in the south flank of EAJ and decelerates westerly in the north flank. Thus, EAJ shifts southward. In contrast, the EAJ shifts northward when the TIO SST is lower than normal.

KEY WORDS tropical Indian Ocean SST; East Asia jet; meridional displacement; the Pacific-Japan/East Asia-Pacific teleconnection

Received 12 October 2010; Revised 25 January 2011; Accepted 5 May 2011

1. Introduction

In the upper and lower stratosphere, there exists a strong westerly belt over the mid-latitudes of East Asia, which is referred to as East Asia westerly jet (EAJ). During boreal summer, the axis of EAJ experiences a northward jump (Yeh *et al*., 1958; Li *et al*., 2004). However, the extent of the northward jump varies from year to year (Liang and Wang, 1998; Lau *et al*., 2000; Lu, 2004). This is related to the year-to-year change in the location of the EAJ or the meridional displacement of EAJ on interannual time scales. Analysis shows that the meridional displacement in the EAJ (MDE) is characterized well by the dominant mode of the zonal wind anomalies in the upper troposphere (Lin and Lu, 2005).

Previous studies noticed that the year-to-year variability of the EAJ is closely linked to monsoon precipitation over East Asia (Liang and Wang, 1998) and downstream climate (Lau and Weng, 2002; Lau *et al*., 2005). During June–August, a southward (northward) displacement of EAJ leads to an increase in precipitation over south-central (north) China (Liang and Wang, 1998). Lau and Weng (2002) indicated that the MDE is associated with North America rainfall. Furthermore, the convection over the western North Pacific (WNP) can affect the MDE through meridional teleconnection (Lau *et al*., 2000; Lu, 2004). However, the variation of convection over the WNP is mainly attributed to the tropical Indian Ocean (TIO) sea surface temperature (SST; Yang *et al*., 2007; Xie *et al*., 2009; Chowdary *et al*., 2010; Chowdary *et al*., 2011).

Owing to the thermocline shoaling in the southwest TIO and the strengthening of ENSO intensity, interannual variability of TIO SST is intensified after the late 1970s (Huang *et al*., 2010; Xie *et al*., 2010). During this epoch, the TIO warms in response to El Niño, and this warming then influences the climate in the Indian Ocean (IO) and surrounding regions after El Niño decays (Yang *et al*., 2007; Xie *et al*., 2009). This phenomenon is referred to as the "capacito' effect'. Through Kelvin wave-induced

* Correspondence to: Gang Huang, RCE-TEA, Institute of Atmospheric Physics, Chinese Academy of Sciences, Beijing 100029, China. E-mail: hg@mail.iap.ac.cn

Ekman divergence (WIED), the capacitor effect can affect the convection over the WNP (Xie *et al*., 2009).

Therefore, there may be a link between the interannual variability of TIO SST and MDE. The aim of this present study is to explore this possible link.

2. Data

This study uses the Hadley Center Global Sea Surface Temperature dataset (Rayner *et al*., 2006), the Center for Climate Prediction Merged Analysis of Precipitation (CMAP; Xie and Arkin, 1997), and the National Centers for Environmental Prediction–National Center for Atmosphere Research atmospheric reanalysis dataset (Kalnay *et al*., 1996). The present analysis will focus on the period 1979–2007 when all the above data are available.

The aim of the present study is to investigate the effects of TIO SST on EAJ on interannual time scales. Linear trends of all the time series have been removed to eliminate decadal and longer time scale variations. Three-month mean is calculated for all variables to remove the intraseasonal variability.

3. Linkage between TIO and meridional displacement of EAJ

A TIO SST index is defined using the area mean SST over the domain of 20 °S–20 °N and 40°–100 °E (shown in Figure 1(a)) in boreal summer. The high TIO SST index corresponds to a significant basin-wide warming in the Indian Ocean (Figure 1(a)), the SST anomalies are about 0.1 ∼ 0.3 K. The relatively warm areas are mainly located in tropical western IO. The precipitation above is not uniform, but the total precipitation is above average, indicating that the TIO warming is not the response to change in atmosphere over it. Though a little weak, the SST anomalies (SSTA) can exert influences on the climate over the TIO and its surrounding regions (e.g. Annamalai *et al*., 2005; Yang *et al*., 2007; Xie *et al*., 2009).

When TIO is warmer than normal, significant warming is found in South China Sea and north of Philippines Sea (Figure 1(a)). Although the warming is embedded in warm pool, the decreased local precipitation (Figure 1(b)) do not support that it is the result of the local warming anomaly. The opposite sign in SST and precipitation anomalies implies that the atmosphere anomalies over WNP are subject to remote forcing, rather than a local one (Wang *et al*., 2005; Xie *et al*., 2009). Thus, the significant warming over WNP contributes little to atmosphere change above.

In addition, significant cooling occurs over north Pacific, east of Japan (Figure 1(a)). Similarly, the opposite sign between SST and local rainfall (Figure 1(b)) suggests that the cooling exerts very little influence on atmosphere change.

The linkage between the TIO SST and the MDE appears significant. The MDE is defined using the first

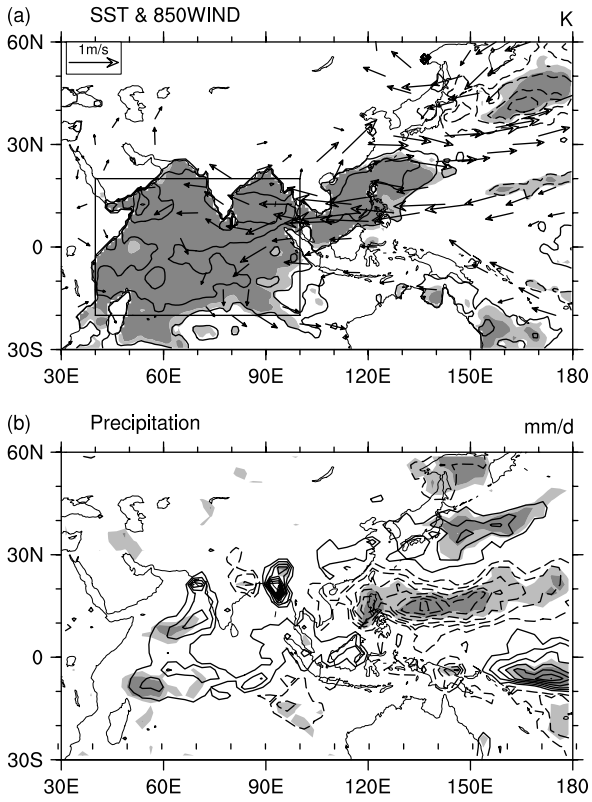

Figure 1. Regression of normalized tropical Indian Ocean (TIO) SST in boreal summer: (a) SST (contours, interval: 0.1 K) and 850 hPa wind (vectors); (b) precipitation (contours, interval: 0.25 mm/d). Light and dark shades in (a) and (b) denote the significance levels are at 95 and 99%, respectively. Only vectors whose significant level exceeds 95% are shown in (a). Contours for zero are omitted.

mode of empirical orthogonal function (EOF) decomposition of summer mean 200 hPa zonal wind in the domain of 27.5°–55 °N and 120°–150 °E, which is the same as that in Lin and Lu (2005). The results (Figure 2) of EOF analysis for 1979–2007 are consistent with those obtained by Lin and Lu (2005). The correlation coefficient of MDE with the TIO SST index is 0.45, exceeding the 95% confidence level. By contrast, the EAJ intensity, which is depicted by the second mode of the EOF results (Lin and Lu, 2005), is poor correlated with TIO SST (the correlation coefficient is −0.28, not reaching 90% significance level).

When the TIO is warm (cold), the ridge of EAJ moves south (north). According to time serial of TIO SST in boreal summer, warm (1983, 1987, 1988, and 1998) and cold (1984, 1985, 1989, and 2000) cases are selected when TIO SST exceeds 1 and −1 standard deviation, respectively. Figure 3(a) and (b) shows the composite results of the warm and the cold cases, respectively. As TIO is warm, the latitude of EAJ ridge is about 38.5–40.5 °E; the latitude is 40–42.5 °E when TIO is cold, a little north compared to the warm cases. Two particular years, 1983 and 1984, are chosen to see the EAJ response. In the summer of 1983, the TIO SSTA is 0.54 K, the EAJ ridge shifts southward (Figure 3(c); 38–40 °E) relative to the average of the warm cases; while during the summer of 1984, the TIO

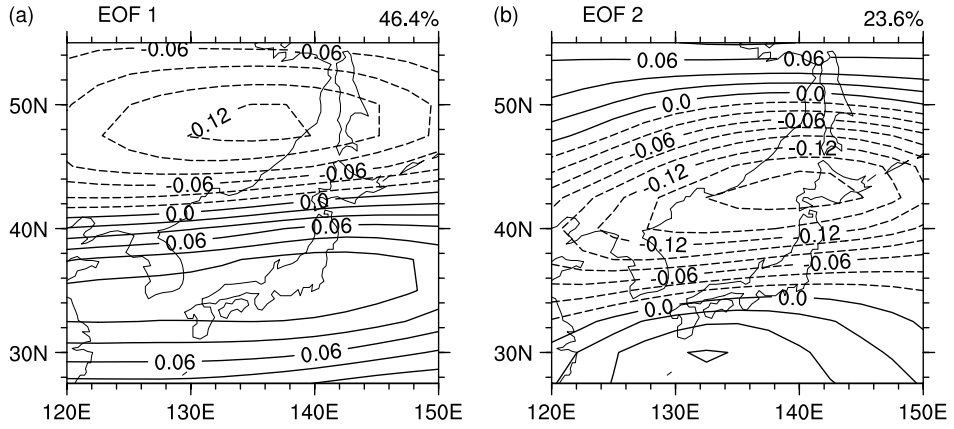

Figure 2. The two modes of EOF decomposition of summer mean zonal wind at 200 hPa, the variance contribution of the two modes are 46.4 and 23.6%, respectively.

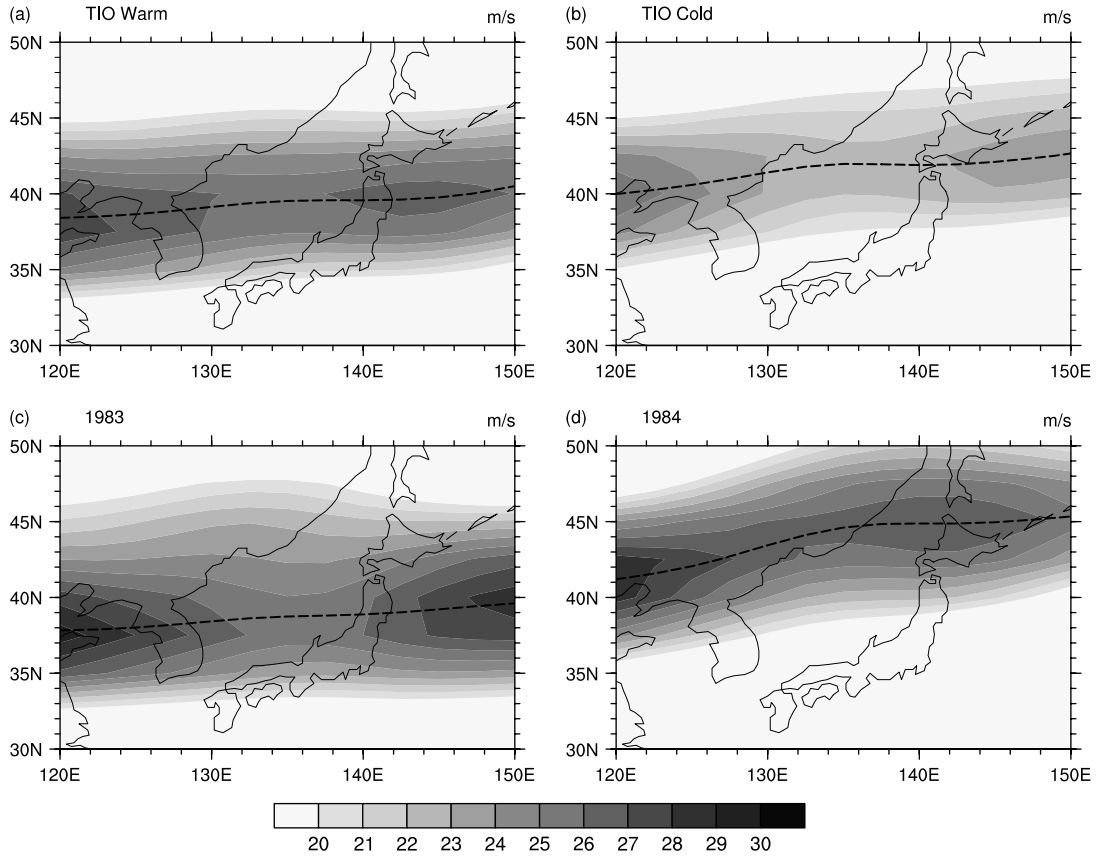

Figure 3. Zonal wind at 200 hPa: (a) and (b) are the results when TIO are warm and cold, respectively. (c) and (d) are the results of 1983 and 1984, respectively. Dash contours in the four plots are the ridge of East Asia Jet.

SSTA is −0.25 K, the EAJ is further north (Figure 3(d); 41–45.5 °E) than that of cold cases mean.

Figure 4 shows the regression of 200 hPa wind vectors on normalized TIO SST index in boreal summer. When the TIO is warmer, there exists an anomalous westerly belt over 200 hPa that extends from North Africa to East Asia. Anomalous easterlies exist over the Okhotsk Sea and to the east of Philippines. Note that over East Asia, the westerly anomaly resides near the south edge of summer mean location of EAJ, and anomalous easterly locates to the north of the belt. This indicates that the westerly jet is strengthened in its southern portion but weakened in its northern portion. Thus, the EAJ shifts southward.

Figure 5 shows the latitude-height sections of zonal wind anomalies obtained by regression on normalized TIO SST index in boreal summer. The four sections (105 °E, 120 °E, 135 °E, and 150 °E) all show anomalous westerlies in the southern part of the westerly jet stream. In the 105 °E section, the westerly maximum locates at

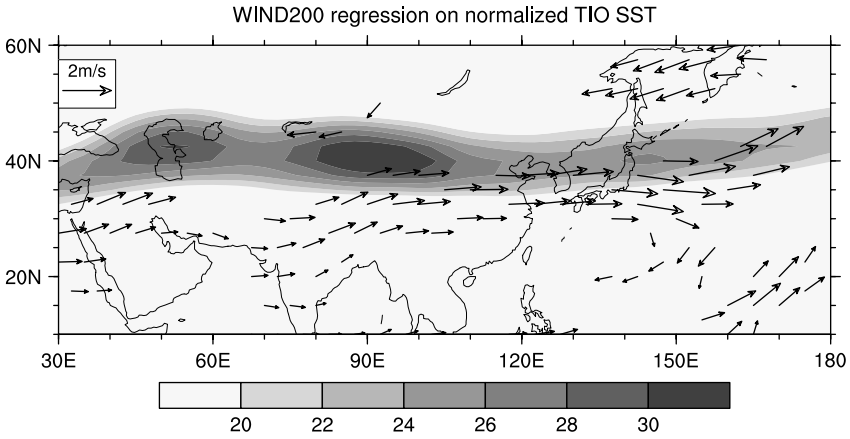

Figure 4. Regression of 200 hPa wind (vectors) on normalized TIO SST in boreal summer, only vectors whose confidence level reaching 95% are shown. Shade shows the climatological zonal wind in boreal summer.

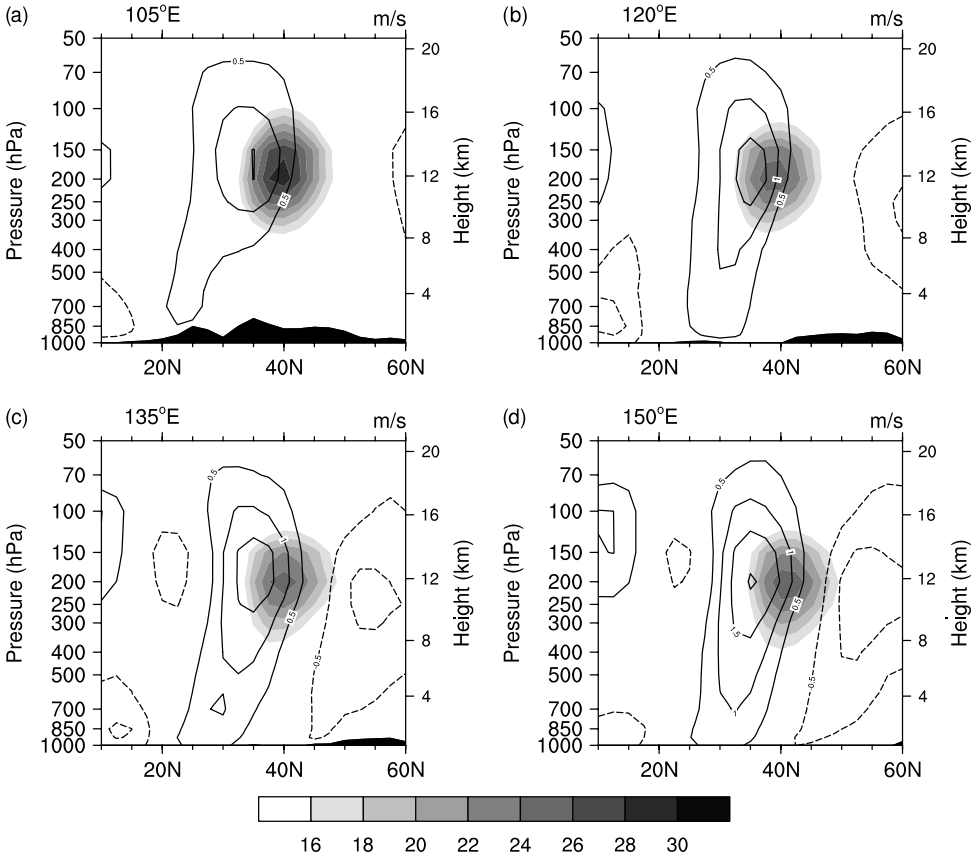

Figure 5. Latitude-height sections of the regression of zonal wind (contours) on normalized TIO SST in boreal summer. The contour interval is 0.5 m/s and the zero contours are omitted for clarity. Shades show the climatological zonal wind in boreal summer, the unit is m/s. (a) is the result of 105 °E section and (b), (c), (d) are the results of 120 °E, 135 °E, 150 °E, respectively. The black areas show the topography height.

150 to 200 hPa. In the other three sections, the maxima are observed at 200 hPa. Over East Asia, especially along 135°–150 °E, the zonal wind anomalies exhibit a Rossby wave-like structure, with negative, positive and negative anomalies from subtropics to mid-latitudes. In addition, the anomalies display poleward tilt with height.

Therefore, in the years when a basin-wide warming occurs in the TIO in boreal summer, the EAJ tends to shift southward. In addition, over East Asia, the zonal wind anomalies exhibit Rossby wave-like structure with a poleward tilt from surface to tropopause.

4. Possible mechanism

The zonal wind anomalies are in good relationship with the anomalous geopotential height. In subtropics and mid-latitudes, wind and geopotential height follow the quasi-geostrophic equilibrium. It means that the zonal wind anomalies are determined by the meridional gradient

of geopotential height anomalies. Figure 6(a) shows the meridional gradient of geopotential height anomalies and wind anomalies at 200 hPa obtained by regression on the TIO SST index. When the TIO SST index is high, the IO is warm, obvious negative meridional gradient of geopotential height anomalies extends from Middle East to the east of Japan and positive gradient is located over the Okhotsk Sea. In Northern Hemisphere, over the areas where the meridional gradient is negative, there exist anomalous easterlies; vice versa, anomalous westerlies exist over the areas where the meridional gradient is positive.

How the TIO warming affects the geopotential height anomalies at 200hPa (hereafter H200)? H200 anomalies are in proportion to the averaged temperature from atmospheric boundary layer (ABL) to 200hPa. Since the temperature in ABL is noisy, the tropospheric temperature (TT; average air temperature between 200hPa and 850hPa) is analysed. When the TIO is warm, a significant tropospheric warming is observed (Figure 6(b)). On the north flank of the TIO warming, significant anomalous westerlies occur due to the warming-induced H200 meridional gradient anomalies (Figure 6(a)). To the east of the TIO, TT exhibits a Kelvin wave-like wedge penetrating into the western Pacific, consistent with the response to localized heating in the TIO (Gill, 1980). Tropical convection modulates TT that is close to a moist-adiabatic profile, which is determined by the equivalent potential temperature in ABL (Emanuel *et al*., 1994, 1997; Su and Neelin, 2003). Through the convection, TIO warming heats the troposphere (Su *et al*., 2003; Xie *et al*., 2009; Huang *et al*., 2010) and forces a Kelvin wave to the east (Neelin and Su, 2005; Xie *et al*., 2009). To the northeast of the TIO, a warm tongue penetrates to the south of Japan from the Bay of Bengal (Figure 6(b)). In addition, there exists a cold centre over the north of Japan. The warm tongue and cold center generate great meridional gradient in H200, which is the key to the intensified westerly over Japan and the weakened westerly to the north of Japan. However, results given by Gill (1980) do not support that the warm tongue and cold center are direct response to the TIO warming (Figure 1(b) given by Gill (1980)). As such, heating over the TIO is not directly responsible for the MDE. Thus, some other processes may act as a bridge connecting TIO heating and EAJ change.

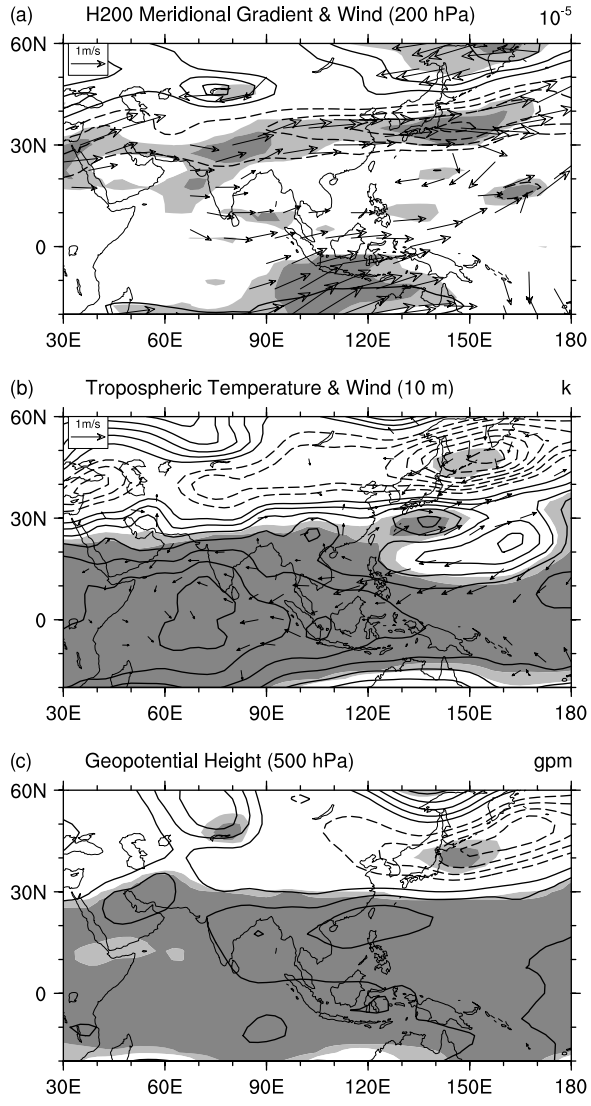

Figure 6. Regression on TIO SST index in boreal summer: (a) meridional gradient of geopoetential height (contours, interval: 5×10^{-6}) and wind (vectors) at 200 hPa; (b) tropospheric temperature (contours, interval: 0.04 k) and 10 m wind (vectors); (c) geopotential height at 500 hPa (contours, interval: 2 gpm). Dash contours indicate the values are negative. For clarity, zero contours are omitted and only vectors whose significant level exceeds 95% are shown. Light and dark shades indicate confidence levels at 95 and 99%, respectively.

When TIO warms, the convection is suppressed near the Philippines by the TIO warming induced-Kelvin wave through the WIED proposed by Xie *et al*. (2009). The suppressed convection can induce an increase in geopotential heights over and to northwest (Figure 6(c)). Near the Philippines, there is climatological easterly shear (the area mean of zonal wind difference between 850 and 200 hPa in the domain of $10^{\circ}-20^{\circ}$N and $110^{\circ}-150^{\circ}$E is 5.1 m/s in boreal summer). With the background easterly shear and the anomalous convection, Rossby wave is generated at low-level and propagates poleward (Lim and Chang, 1983, 1986; Wang and Xie, 1996; Lu, 2004). The wind anomalies at 850 hPa (Figure 1(a)) display a wave pattern over the coast of East Asia. Thus, the PJ teleconnection (Nitta, 1987) or the East Asian-Pacific (EAP) teleconnection (Huang and Sun, 1992) is prominent (Figures 1(b) and 6(c)). The correlation coefficients of the PJ index (Wakabayashi and Kawamura, 2004) and the EAP index (Huang and Yan, 1999) with the TIO SST index are -0.57 and -0.55, respectively, both exceeding the 99% confidence level.

The PJ/EAP teleconnection has a unique vertical structure. Kosaka and Nakamura (2006) found the PJ teleconnection pattern not only exists at lower level, but also at upper level. In addition, their study showed that the teleconnection pattern tilts northward with height. Our analysis confirms these results (Figure 5). Anomalous precipitation near Japan and the vertical structure of the

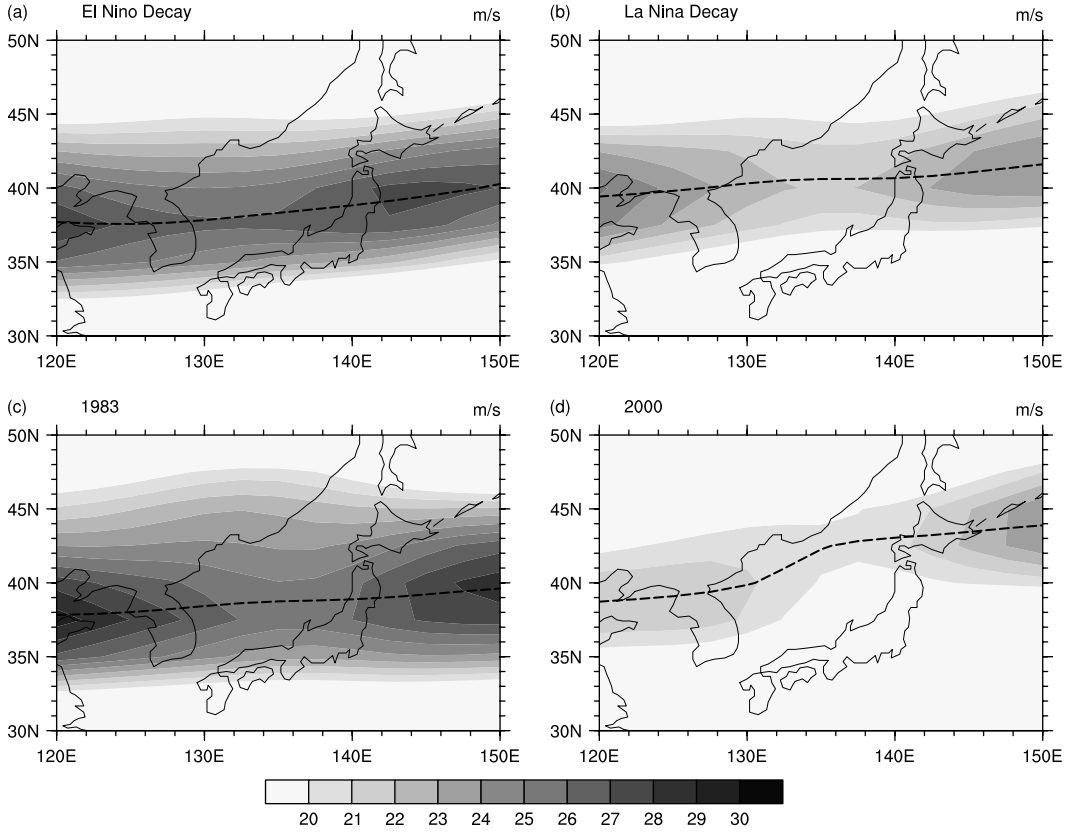

Figure 7. The same as Figure 3, except for: (a) and (b) are the results when El Niño and La Niña Decay, respectively. (c) and (d) are the results of 1983 and 2000, respectively.

mean flow may be responsible for the tilt (Kosaka and Nakamura, 2006; Lu and Lin, 2009). Thus, over the coast of East Asia, the mid-latitude cyclonic wind anomalies at upper level are slightly poleward in comparison to those at low level (Figure 1(a) andFigure 4). The anomalous winds can also be interpreted as the results of the PJ/EAP pattern-induced H200 anomalies.

Interestingly, the zonal wind is more obvious east of 120 °E in mid-latitude. It may be the combined effects of WNP rainfall induced-EAP/PJ teleconnection and the precipitation east of Japan. The teleconnection mainly locates east of 120 °E (Figures 1(b) and 6(c)). The corresponding positive and negative height anomalies at upper level (can be inferred by the TT regression result in Figure 6(b)), which is also east of 120 °E, may cause great meridional gradient between them and lead to relative strong anomalous zonal wind. Indeed, such anomalies couple the effects of the precipitation east of Japan. Simulation results in Lu and Lin (2009) suggest that the precipitation is able to generate such zonal wind anomalies.

5. Conclusions and discussions

When the TIO warms in boreal summer, significant warming is found in the South China Sea and north of Philippines Sea, and cooling exists in east of Japan. The local rainfall over those areas is in opposite sign with the SSTAs, suggesting that little influence do the SSTAs exert on local atmosphere change.

As TIO warms (cools), the ridge of EAJ moves southwards (northwards). It is the result of westerly strengthening (weakening) in the south flank of EAJ's climatological location and the deceleration (acceleration) of westerly in the north. In addition, over the coast of East Asia, the anomalous zonal winds in troposphere exhibit a Rossby wave-like structure from subtropics to mid-latitude and the anomalies tilt poleward with height.

Furthermore, the mechanism how the interannual variability of TIO SST affects the meridional displacement of EAJ is investigated. Here, we summarize the possible mechanism as follows: As TIO warms, anomalous convection over the TIO leads to the tropospheric warming and forces a Kelvin wave wedge penetrating into the equatorial western Pacific (Xie *et al*., 2009). The Kelvin wave-induced Ekman divergence suppresses convection over the WNP (Xie *et al*., 2009). The decreased precipitation under climatological easterly shear forces the PJ/EAP teleconnection (Lu, 2004). The teleconnection-associated cyclonic wind at upper level over Japan, intensifies westerly in the south part of EAJ and weakens westerly in the north part of EAJ. Thus, EAJ shifts southward.

Interestingly, the anomalous zonal wind is more obvious east of 120 °E in mid-latitude, it may be caused by

the WNP rainfall-induced EAP/PJ teleconnection and the rainfall anomalies mainly locate east of 120 °E.

Similar to the composite analysis in Section 3, the relationship between the EAJ ridge and ENSO is analysed. El Niño (1982–1983, 1991–1992, 1997–1998) and La Niña (1984–1985, 1988–1989, 1999–2000) cases are selected based on ±1 standard deviation. The ridge is about 37.5–40.5 °E in the El Niño cases mean and shifts a little further southward in 1983, one of the El Niño decaying years (Figure 7(a) and (c)). The ridge is about 39.5–41.5 °E in the La Niña cases mean (Figure 7(b)). While, in one of the La Niña decaying year, 2000, the ridge tilts northeastwards (Figure 7(d)). It locates in 39–44 °E, its mean latitude shift northwards relative to that in the La Niña cases mean. The results are similar to those of the TIO SST in Section 3. The correlation coefficient between TIO SST and ENSO is 0.80 for the period from 1979–2007. This accounts for the similarity.

Though highly affected by ENSO, the TIO SST does have impacts on western WNP precipitation, which in turn leads to the movement of the westerly jet. Serials of studies found that the TIO warming is triggered by ENSO and that the warming is induced by ocean dynamics and local air–sea interaction (Huang and Kinter, 2002; Xie *et al*., 2002; Du *et al*., 2009; Xie *et al*., 2009). Indeed, ENSO does not affect the WNP rainfall directly and that ENSO-induced TIO SSTA in the following summer is an important direct factor (Yang *et al*., 2007; Xie *et al*., 2009; Chowdary *et al*., 2010, 2011). A coupled general circulation model, which has quite good predicting skill, is used to analyse the relative role of TIO (Chowdary *et al*., 2011). The results showed that the TIO warming accounts for 50% of the anomalous sea level pressure over WNP and helps the lower level anomalous anticyclone to expand westward through the South China Sea in the summer after El Niño decays. Therefore, though not the only factor, the TIO warming plays a very important role in WNP circulation change. In addition, muti-model results confirm the aforementioned conclusion (Chowdary *et al*., 2010).

Acknowledgements

The authors are grateful to two anonymous reviewers for their valuable comments that helped to improve our manuscript. This study was supported by the CAS XDA05090402, the Special Scientific Research Project for Public Interest (Grant No. GYHY201006021), the National Basic Research Program of China (2011CB 309704), the Third Institute of Oceanography State Oceanic Administration GCMAC1007, the National Natural Science Foundation of China under Grants (Nos. 40890155, U0733002, 40810059005).

References

Annamalai H, Liu P, Xie SP. 2005. Southwest Indian Ocean SST Variability: Its Local Effect and Remote Influence on Asian Monsoons. *Journal of Climate* **18**: 4150–4167.

Chowdary JS, Xie SP, Lee J, Kosaka Y, Wang B. 2010. Predictability of summer northwest Pacific climate in 11 coupled model hindcasts: Local and remote forcing. *Journal of Geophysical Research* **115**: D22121, DOI:10.1029/2010JD014595.

Chowdary JS, Xie SP, Luo J, Hafner J, Behera S, Masumoto Y, Yamagata T. 2011. Predictability of Northwest Pacific climate during summer and the role of the tropical Indian Ocean. *Climate Dynamics*, DOI:10.1007/s00382-009-0686-5 (in press).

Du Y, Xie SP, Huang G, Hu K. 2009. Role of Air–Sea Interaction in the Long Persistence of El Niño–Induced North Indian Ocean Warming. *Journal of Climate* **22**: 2023–2038.

Emanuel KA, Neelin JD, Bretherton CS. 1994. On large-scale circulations in convecting atmospheres. *Quarterly Journal of the Royal Meteorological Society* **120**: 1111–1143.

Emanuel KA, Neelin JD, Bretherton CS. 1997. Reply to comments by Bjorn Stevens, David A. Randall, Xin Lin, Michael T. Montgomery on 'On large-scale circulations in convecting atmospheres.'. *Quarterly Journal of the Royal Meteorological Society* **123**: 1779–1782.

Gill AE. 1980. Some simple solutions for heat-induced tropical circulation. *Quarterly Journal of the Royal Meteorological Society* **106**: 447–462.

Huang G, Hu K, Xie SP. 2010. Strengthening of tropical Indian Ocean teleconnection to the Northwest Pacific since the mid-1970s: An atmospheric GCM study. *Journal of Climate* **23**: 5294–5304.

Huang B, Kinter JL. 2002. Interannual variability in the tropical Indian Ocean. *Geophysical Research Letters* **107**: 3199, DOI:10.1029/2001JC001278.

Huang G, Qu X, Hu K. 2010. The impact of the tropical Indian Ocean on the South Asian High in boreal summer. *Advances In Atmospheric Sciences*. DOI:10.1007/s00376-010-9224-y, in press.

Huang G, Yan Z. 1999. The East Asian summer monsoon circulation anomaly index and the interannual variations of the East Asian summer monsoon. *Chinese Science Bulletin* **44**: 1325–1329.

Huang R, Sun F. 1992. Impact of the tropical western Pacific on the East Asian summer monsoon. *Journal of the Meteorological Society of Japan* **70**: 243–256.

Kalnay E, Kanamitsu M, Kistler R, Collins W, Deaven D, Gandin L, Iredell M, Saha S, White G, Woollen J. 1996. The NCEP/NCAR 40-year reanalysis project. *Bulletin of the American Meteorological Society* **77**: 437–471.

Kosaka Y, Nakamura H. 2006. Structure and dynamics of the summertime Pacific-Japan (PJ) teleconnection pattern. *Quarterly Journal of the Royal Meteorological Society* **132**: 2009–2030.

Lau KM, Kim KM, Yang S. 2000. Dynamical and boundary forcing characteristics of regional components of the Asian summer monsoon. *Journal of Climate* **13**: 2461–2482.

Lau KM, Weng H. 2002. Recurrent teleconnection patterns linking summertime precipitation variability over East Asia and North America. *Journal of the Meteorological Society of Japan* **80**: 1309–1324.

Lau NC, Leetmaa A, Nath MJ, Wang HL. 2005. Influences of ENSO-induced Indo-Western Pacific SST anomalies on extratropical atmospheric variability during the boreal summer. *Journal of Climate* **18**: 2922–2942.

Li C, Wang Z, Lin S, Cho H. 2004. The relationship between East Asia summer monsoon activity and northward jump of the upper westerly jet location. *Chinese Journal of Atmospheric Sciences* **28**: 641–658 (in Chinese).

Liang XZ, Wang WC. 1998. Association between China monsoon rainfall and tropospheric jets. *Quarterly Journal of the Royal Meteorological Society* **124**: 2597–2623.

Lim H, Chang CP. 1983. Dynamics of teleconnections and Walker Circulations forced by equatorial heating. *Journal of Atmospheric Sciences* **40**: 1897–1915.

Lim H, Chang CP. 1986. Generation of internal-and external-mode motions from internal heating: effects of vertical shear and damping. *Journal of Atmospheric Sciences* **43**: 948–960.

Lin Z, Lu R. 2005. Interannual meridional displacement of the East Asian upper-tropospheric jet stream in summer. *Advances In Atmospheric Sciences* **22**: 199–211.

Lu R. 2004. Associations among the components of the East Asian summer monsoon system in the meridional direction. *Journal of the Meteorological Society of Japan* **82**: 155–165.

Lu R, Lin Z. 2009. Role of subtropical precipitation anomalies in maintaining the summertime meridional teleconnection over the western North Pacific and East Asia. *Journal of Climate* **22**: 2058–2072.

Neelin JD, Su H. 2005. Moist Teleconnection Mechanisms for the Tropical South American and Atlantic Sector. *Journal of Climate* **18**: 3928–3950.

Nitta T. 1987. Convective activities in the tropical western Pacific and their impact on the northern hemisphere summer circulation. *Journal of the Meteorological Society of Japan* **65**: 373–390.

Rayner NA, Brohan P, Parker DE, Folland CK, Kennedy JJ, Vanicek M, Ansell TJ, Tett SFB. 2006. Improved snalyses of changes and uncertainties in sea surface temperature measured in situ since the mid-nineteenth century: The HadSST2 dataset. *Journal of Climate* **19**: 446–469.

Su H, Neelin JD. 2003. The scatter in tropical average precipitation anomalies. *Journal of Climate* **16**: 3966–3977.

Su H, Neelin JD, Meyerson JE. 2003. Sensitivity of Tropical Tropospheric Temperature to Sea Surface Temperature Forcing. *Journal of Climate* **16**: 1283–1301.

Wakabayashi S, Kawamura R. 2004. Extraction of major teleconnection patterns possibly associated with the anomalous summer climate in Japan. *Journal of the Meteorological Society of Japan* **82**: 1577–1588.

Wang B, Ding Q, Fu X, Kang I, Jin K, Shukla J, Doblas-Reyes F. 2005. Fundamental challenge in simulation and prediction of summer monsoon rainfall. *Geophysical Research Letters* **32**: L15711, DOI:10.1029/2005GL022734.

Wang B, Xie X. 1996. Low-frequency equatorial waves in vertically sheared zonal flow. Part I: stable saves. *Journal of Atmospheric Sciences* **53**: 449–467.

Xie P, Arkin PA. 1997. Global precipitation: a 17-year monthly analysis based on gauge observations, satellite estimates, and numerical model outputs. *Bulletin of the American Meteorological Society* **78**: 2539–2558.

Xie SP, Annamalai H, Schott FA, McCreary JP. 2002. Structure and Mechanisms of South Indian Ocean Climate Variability. *Journal of Climate* **15**: 864–878.

Xie SP, Du Y, Huang G, Zheng XT, Tokinaga H, Hu K, Liu Q. 2010. Decadal shift in El Niño influences on Indo-western Pacific and East Asian climate in the 1970s. *Journal of Climate* **23**: 3352–3368.

Xie SP, Hu K, Hafner J, Tokinaga H, Du Y, Huang G, Sampe T. 2009. Indian Ocean Capacitor Effect on Indo-Western Pacific climate during the summer following El Niño. *Journal of Climate* **22**: 730–747.

Yang J, Liu Q, Xie SP, Liu Z, Wu L. 2007. Impact of the Indian Ocean SST basin mode on the Asian summer monsoon. *Geophysical Research Letters* **34**: L02708, DOI:10.1029/2006GL028571.

Yeh DZ, Tao SY, Li MC. 1958. The abrupt change of circulation over Northern Hemisphere during June and October. *Acta Meteorological Sinica* **29**: 250–263 (in Chinese).

